ORIGINAL RESEARCH

Activating Transcription Factor 6 Mediates Inflammation in Experimental Varicocele-Induced Epididymal Epithelial Cells

Yin-shan Jin*, Yuan-qing Cui*, Yan-ping Xu*, Jie Chen, Xue-bao Zhang, Xiong Wang 🆔

Department of Reproductive Medicine, Yantai Yuhuangding Hospital, Yantai, 264000, People's Republic of China

*These authors contributed equally to this work

Correspondence: Xiong Wang, Department of Reproductive Medicine, Yantai Yuhuangding Hospital, No. 20, Yuhuangding East Road, Yantai, 264000, People's Republic of China, Email wangxiong01903@163.com

Introduction: Varicocele is a dilatation of the internal spermatic vein and it is generally recognized as one cause of male infertility. This study aimed to analyze the roles of activating transcription factor 6 (ATF-6) in experimental varicocele-induced epididymal epithelial cells.

Methods: Experimental left varicocele was established in rats through partial left renal vein ligation. At 8 weeks after surgery, the left epididymal damage was observed using H&E and TUNEL staining. The expressions of neutral α-glucosidase (NAG), ATF-6, tumor necrosis factor (TNF)-α, and phospho-nuclear factor (p-NF)-κB p65 (S536) in the left epididymis were measured by immunohistochemistry. ATF-6 silence in rat epididymal epithelial cells was established by ATF-6 siRNA transfection. The cells were treated with hypoxia for 24 h, and cell viability was measured by CCK-8, levels of NAG, TNF-α, and interleukin (IL)-8 in cells were measured by ELISA, levels of p-NF-κB p65 (S536)/NF-κB p65 protein in cells were measured by Western blotting.

Results: The results showed that the experimental left varicocele induced hypertrophy and apoptosis of epididymal epithelial cells ($p<0.05$), and decreased the expressions of NAG in the epididymal epithelial cells compared with the sham-operated control rats ($p<0.01$). Meanwhile, the expressions of ATF-6, TNF-α, and p-NF-κB p65 (S536) were increased in the epididymal epithelial cells after the experimental left varicocele compared with the sham-operated control rats ($p<0.05$). In the hypoxia-treated cells, ATF-6 silence increased the cell viability and decreased the levels of TNF-α, IL-8, and p-NF-κB p65 (S536) compared with the control cells ($p<0.05$).

Discussion: The ATF-6 pathway was activated in a rat's left varicocele-induced epididymal damage. Inhibition of the ATF-6 pathway might be a possible novel therapeutic approach for left varicocele-induced epididymal damage.

Keywords: epididymal neutral α-glucosidase, hypoxia, left varicocele, nuclear factor-kappa B p65, NF-κB p65

Introduction

Varicocele is an abnormal dilatation, elongation, and tortuosity of the pampiniform plexus veins of the spermatic cord, occurring on the left side.[1,2] It is generally reported that varicocele is present in 15% of the general male population and accounts for about 35% of men with primary infertility, and 70–85% of men with secondary infertility, making it the most common cause of male infertility.[1,3] Various surgical techniques, including different types of open varicocelectomy and minimally invasive techniques, such as microsurgical, microscopic laparoscopic, laparoscopic or robotic varicocelectomy, can be used to treat varicocele with high success rates.[4] Removal of varicocele in mature men improves semen parameters in over 50% of men, or if treated in adolescence, in over 80% of adolescents.[5] However, over 60% of couples with infertility and varicocele do not have spontaneous pregnancy within a year after varicocelectomy, and one factor contributing to this outcome may be epididymal damage.[6] Therefore, varicocele-induced epididymal damage is an important issue in male infertility.

Epididymis is a key organ for sperm maturation and fertilization capacity, and it is responsible for sperm storage and transport.[7] It has been reported that the varicocele can induce cell apoptosis in the epididymal epithelium,[6] degeneration of the epididymal epithelium,[8] and decrease the secretion of epididymal neutral α-glucosidase (NAG).[9] The levels of NAG are almost exclusively in the epididymis and are useful for epididymal function, mainly localized in the apical cytoplasm.[9,10] It has been shown that varicocele-mediated infertility is the result of the synergy of genetic and other molecular factors, such as scrotal hyperthermia, hypoxia, inflammation, endocrine disorders, and oxidative stress.[2,11] However, most studies examining the association between varicocele and fertility are principally focused on the damage to the testis. In fact, the epididymal dysfunction is associated with varicocele-related male infertility. The mechanisms of pathophysiology of varicocele-induced epididymis are needed to be elucidated.

As known, varicocele is frequently accompanied by an accumulation of unfolded or misfolded proteins, indicating impaired endoplasmic reticulum (ER) function.[12] In a rat varicocele testis model, ER stress and unfolded protein response (UPR) occurred in the testis as evidenced by the engagement of the IRE1/JNK/XBP1s pathway and caspase-3-mediated apoptosis.[11] The ER stress is a protective response to restore protein homeostasis by activating the UPR. However, severe and/or persistently high ER stress can trigger cell apoptosis through multiple inflammatory pathways, such as the PI3K-Akt pathway, nuclear factor (NF)-κB pathway, and nod-like receptor family pyrin domain containing 3 (NLRP3) inflammasome.[13,14] Activating transcription factor 6 (ATF-6) is a transduction molecule in the downstream signal pathway of UPR, that can combine with the ER stress response element (ERSE) to regulate the homeostasis of ER and maintain cell functions.[15] In inflammatory diseases, the ATF-6 expressions increased and promoted the secretions of inflammatory cytokines and ER stress-mediated apoptosis.[16–18] However, the ATF-6 expression in the varicocele-induced epididymal dysfunction has not been reported. Exploring the implications of ATF-6 in varicocele-induced epididymal dysfunction is crucial for developing potential therapeutic interventions.

In this study, a rat model of left varicocele was established by partial left renal vein ligation. The expressions of ATF-6, TNF-α, and phospho-NF-κB p65 (S536) were observed in the varicocele-induced epididymis. In rat epididymal epithelial cells, cells were treated with hypoxia to mimic varicocele-induced epididymis in vitro, and the roles of ATF-6 silence in inflammation were observed in the hypoxia-stimulated cells.

Materials and Methods
Sample Size Calculation
The sample size was calculated using G*Power 3.1 software (Franz, Universitat Kiel, Germany). With power of 70%, 0.05 level of statistical significance, and effect size of 0.6, total sample size was calculated to be 11. Twelve animals were used in this study.

Animals and Animal Group
Twelve adult male Sprague-Dawley rats (250–300 g, 7 weeks) were purchased from Ji'nan Pengyue Laboratory Animal Breeding Co., Ltd. (Shandong, China) and maintained under a controlled environment at 20–22°C, with 45–55% humidity, and a 12-hour light-dark cycle. All rats were fed water and standard rodent feed. Animals were randomly divided into the experimental varicocele group (n=6) and the sham-operated control group (n=6).

Experimental Left Varicocele
It should be noted that individual variation is one of the major difficulties of the study of venous anatomy in both humans and laboratory animals. In comparison with the naturally occurring left varicocele in humans, the rat experimental left varicocele causes a redistribution of blood flow from a route primarily out the spermatic vein to routes leading to the iliac vein, and the redistribution is similar but not identical.[19] In this study, experimental left varicocele was established through partial left renal vein ligation.[20] The rats were anesthetized by a 2% pentobarbital sodium (#P3761, Sigma-Aldrich, Shanghai, China) injection, and explored the left renal vein. The left renal vein and a parallel 0.85 mm metal probe were tied using a 4/0 silk ligature (#N180918, Fosun Pharma, Shanghai, China). After removing the probe, an approximate 50% decrease in renal vein diameter was produced. The incision was then closed. Sham-operated (control)

rats were subjected to the same laparotomy but without renal vein ligation. Animals of the two groups were then housed under controlled lighting and temperature conditions.

Sample Collection
At 8 weeks following surgery, all rats were sacrificed by intraperitoneal injection of 100 mg/kg pentobarbital sodium (#P3761, Sigma-Aldrich, Shanghai, China). The left epididymis was isolated by excising the efferent ducts and vas deferens and fixed in 2.5% glutaraldehyde (#G849973, Macklin, Shandong, China) for 24 h.

Histological Observation Using Hematoxylin-Eosin (H&E) Staining and Terminal-Deoxynucleotidyl Transferase-Mediated Nick End Labeling (TUNEL) Staining
H&E Staining
According to the H&E staining procedures,[21] the fixed tissues were treated with gradient ethanol (80%, 90%, 95%, 100%) for 120 min each time at room temperature. Then, the tissues were embedded in paraffin and cut into paraffin sections (4 μm). The sections were dewaxed with xylene twice (5 min each time) and hydrated with gradient ethanol (100%, 90%, 80%, 70%) for 2 min each time at room temperature. After washing with water for 5 min, the sections were stained with hematoxylin (#C0105S, Beyotime, China) for 10 min at room temperature. After washing with water, the sections were differentiated with 1% acid alcohol for the 20s. After washing, the sections were stained with eosin (#C0105S, Beyotime, China) for 1 min. After washing, the sections were treated with gradient ethanol (70%, 80%, 90%, 100%) for 20s each time and xylene twice for 5 min each time at room temperature. The sections were sealed with neutral gum and observed by ×200 magnification under a light microscope (#DM3000, Leica, Germany).

TUNEL Staining
According to the TUNEL apoptosis detection kit instructions (#Alexa Fluor 488, Yeasen, Shanghai, China), the paraffin sections (4 μm) were soaked in xylene for 5 min, and soaked in gradient ethanol (100%, 5 min; 90%, 3 min; 80%, 3 min; 70%, 3 min). After washing with phosphate buffer saline (PBS, #P787575, Macklin, Shandong, China) for 3 min, the sections were cultured with 20 μg/mL Proteinase K (#ST533, Beyotime, Shanghai, China) for 20 min at room temperature. After washing with PBS twice, the sections were cultured with 1× equilibration buffer for 20 min and TdT buffer (#D7092S, Beyotime, Shanghai, China) for 60 min at room temperature. After washing with PBS twice, the sections were treated with gradient ethanol (90%, 95%, 100%) for 2 min each time and xylene twice for 3 min each time at room temperature. The sections were sealed with neutral gum and the numbers of TUNEL-positive cells were observed by ×200 magnification under a light microscope (#DM3000, Leica, Germany).

Immunohistochemistry Analysis of NAG, ATF-6, TNF-α and p-NF-κB p65 Expressions
According to the immunohistochemistry staining procedures,[22] the paraffin sections (4 μm) were dewaxed with xylene twice (5 min each time) and hydrated with gradient ethanol (100%, 90%, 80%, 70%) for 2 min each time at room temperature. Then, the sections were soaked in Proteinase K solution for 6 min at room temperature. After washing with PBS twice, the sections were cultured with 3% H_2O_2 for 15 min at room temperature. After washing with PBS twice, the sections were respectively incubated with primary antibodies (Table 1) overnight at 4°C. After washing with PBS twice, the sections were incubated with the HRP anti-rabbit IgG antibody (1:1000, #ab288151, Abcam, Shanghai, China) for 30 min at 37°C. After washing with PBS twice, the sections were stained with diaminobenzidine (DAB, #AR1022, Boster, Shanghai, China) for 2 min and hematoxylin for 3 min at 37°C. After washing, the sections were dehydrated with gradient ethanol (90%, 95%, 100%) for 2 min each time and cleared with xylene twice for 3 min each time at room temperature. Finally, the sections were sealed with neutral gum. The results were observed by ×200 magnification under a light microscope (#DM3000, Leica, Germany). The positive expression was marked by a brown color and the positive staining area (%) was analyzed using ImageJ software (National Institutes of Health, USA).

Table 1 Information of Primary Antibodies

Antibody	Host	Code	Dilution	Source
NAG	Rabbit	ab133720	1:2000	Abcam, Shanghai, China
ATF-6	Rabbit	ab37149	5 μg/mL	Abcam, Shanghai, China
TNF-α	Rabbit	ab6671	1:800	Abcam, Shanghai, China
Phospho(p)-NF-κB p65 (S536)	Rabbit	ab86299	1:800	Abcam, Shanghai, China

Abbreviations: NAG, neutral α-glucosidase; ATF-6, activating transcription factor 6; TNF-α, tumor necrosis factor-α; NF-κB, nuclear factor-kappa B.

Cells and Cell Culture

Rat epididymal epithelial cells (#CP-R335, Procell Life Science & Technology Co., Ltd, China) were identified with pancytokeratin (PCK, #ab215838, Abcam, Shanghai, China) immunofluorescence (≥90%). The cells were cultured at 37°C with 5% CO_2 using the medium (#CM-R335, Procell, China) containing fetal bovine serum (FBS), epidermal growth factor (EGF), hydrocortisone, adrenaline, thyroid hormone, insulin, transferrin, selenium solution, penicillin, streptomycin. At about 70% confluency, the cells ($2×10^5$ per well) were used for experiments.

Cell Transfection and Cell Group

The cells ($2×10^5$ per well) were cultured in a 24-well plate and transfected with 1 μg small interfering RNA (siRNA) targeting ATF-6 or control siRNA (GenePharma Co., Ltd, Shanghai, China) for 24 h using Lipofectamine 3000 (#L3000150, Invitrogen, Shanghai, China). Briefly, the dilute Lipofectamine™ 3000 reagents (25 μL × 2) were added to Opti-MEM™ medium (0.75 and 1.5 μL, 2 tubes). The master mix of siRNA (1 μg) was diluted in Opti-MEM™ medium (50 μL) and was mixed with P3000™ reagent (2 μL). Then, the diluted siRNA was added to each tube of diluted Lipofectamine™ 3000 reagents (1:1 ratio) for 12 min at room temperature. The cells were incubated with the siRNA-lipid complex for 24 h at 37°C with 5% CO_2. The sequence of ATF-6 siRNA is 5′-CCCUCAUUAACACGACAGATT-3′.

The cells were divided into three groups, the control group, the control siRNA group, and the ATF-6 siRNA group. Three repeats per group in each experiment.

Assessment of ATF-6 siRNA Transfection Using Western Blotting, Cell Counting Kit-8 (CCK-8) and NAG Activity Assay

Western Blotting

The expressions of proteins were measured by Western blotting.[23] Protein extraction was carried out from cells using a lysis buffer, and the protein concentrations were determined by the Bicinchoninic Acid method (#P0012, Beyotime, China). The collected proteins were separated by 12% gel electrophoresis (#P0690, Beyotime, China) and transferred to polyvinylidene fluoride (PVDF) membranes (#FFP70, Beyotime, China). After blocking with 5% milk for 60 min, the membranes were incubated with primary antibodies at 4°C overnight. The antibodies included rabbit polyclonal to ATF-6 (0.5 μg/mL, #ab37149, Abcam, Shanghai, China), rabbit polyclonal to p-NF-κB p65 (S536) (1:2000, #ab86299, Abcam), rabbit polyclonal to NF-κB p65 (0.5 μg/mL, #ab16502, Abcam) and rabbit polyclonal to β-action (1:2000, #ab8227, Abcam). After washing with PBST (10 min each time) three times, the membranes were incubated with the secondary antibody, HRP anti-rabbit IgG antibody (1:2000, #ab288151, Abcam) for 120 min at 37°C. After washing with PBST three times, the membranes were visualized using the enhanced ECL chemiluminescent substrate kit (#3622ES60, Yeasen, Shanghai, China). The gray of proteins was performed using ImageJ software (National Institutes of Health, USA). The relative expression of the protein was normalized using β-action.

CCK-8

The cell viability was measured using a CCK-8 kit (#C0038, Beyotime, Shanghai, China). According to the kit instructions, 10 μL of cells ($2×10^3$ per well) were cultured with 10 μL of CCK-8 for 2 h at 37°C with 5% CO_2. The absorbance was measured at 450 nm using a microplate reader (#Varioskan ALF, Thermo Scientific, China).

NAG Activity Assay

According to the α-glucosidase activity assay kit instructions (#BC2550, Solarbio Science & Technology Co., Ltd, Beijing, China), the cells were collected by centrifugation (500 g, 10 min) using a centrifuge (#Sorvall ST4 plus, Thermo Scientific, China), and crushed in 1 mL of extraction solution using ultrasonic (power 200W, 3s) for 30 times. After centrifugation (15,000 g, 20 min, 4°C), the supernatants were collected and measured at 400 nm using a microplate reader (#Varioskan ALF, Thermo Scientific, China).

Hypoxia Cell Model and Cell Group

Several mechanisms have been proposed to explain the pathophysiology of varicocele, likely scrotal hyperthermia, hypoxia, reflux of renal and adrenal metabolites, and hormonal imbalances.[2] Here, cells were treated with hypoxia to mimic varicocele-induced epididymis in vitro. The cells were cultured at 37°C with 5% CO_2, 2% O_2, and 93% N_2 for 24 h.[24] The control cells were cultured at 37°C with 5% CO_2 for 24 h.

The cells were divided into four groups, the control group, the ATF-6 siRNA group, the hypoxia control group, and the hypoxia plus ATF-6 siRNA group. Three repeats per group in each experiment.

Assessment of ATF-6 Silence Under Hypoxia Using CCK-8, NAG Activity Assay, Enzyme-Linked Immunosorbent Assay (ELISA), and Western Blotting

CCK-8, NAG Activity Assay, and Western Blotting

As described in the above-mentioned methods, CCK-8 measured the cell viability, α-glucosidase activity assay measured the NAG levels, and Western blotting measured the levels of p-NF-κB p65/NF-κB p65 protein.

Elisa

The levels of TNF-α and interleukin (IL)-8 in supernatants of cells were measured using ELISA. According to the rat TNF-α ELISA kit (#PT516, Beyotime, Shanghai, China) and rat IL-8 ELISA kit (#SEKR-0071, Solarbio Science & Technology Co., Ltd, Beijing, China) instructions, the supernatants of cells were collected by centrifugation (500 g, 10 min) using a centrifuge (#Sorvall ST4 plus, Thermo Scientific, China), and the collected supernatants were cultured with biotinylated antibody for 60 min and streptavidin for 20 min at 25°C. Then, the samples were cultured with 3.3′,5,5′-tetramethylbenzidine (TMB) for 20 min at 25°C before the addition of the stop solution. The results were measured at 450 nm using a microplate reader (#Varioskan ALF, Thermo Scientific, China).

Statistics Analysis

The statistics analysis was performed by the GraphPad Prism 8.0 software (GraphPad Software Inc., La Jolla, USA). The normal distribution of data was tested by the Shapiro–Wilk test, and the results were shown as mean ± standard deviation. The t-test was used to compare significance between two groups, and ANOVA with post hoc Tukey's test was used to compare significance among multiple groups. A p-value of < 0.05 was considered as significant.

Results

Epididymal Damage Was Induced by Experimental Left Varicocele

The experimental left varicocele in rats was established through partial left renal vein ligation (Figure 1A). At 8 weeks after surgery, the rats were sacrificed and the left epididymal morphology was observed by H&E staining (Figure 1B). Compared with the control group, the epithelial cell thickness (red arrows) significantly increased in the caput (p=0.027), corpus (p=0.017), and cauda (p=0.026) after the experimental left varicocele (Figure 1C). Meanwhile, the apoptosis of epididymal endothelial cells (red arrows) in the left epididymis was observed by TUNEL staining (Figure 1D). Compared with the control group, the cell apoptosis significantly increased in the caput (p=0.005), corpus (p=0.001), and cauda (p=0.004) after the experimental left varicocele (Figure 1E). The results showed that experimental left varicocele induced damage to the epididymal endothelial cells.
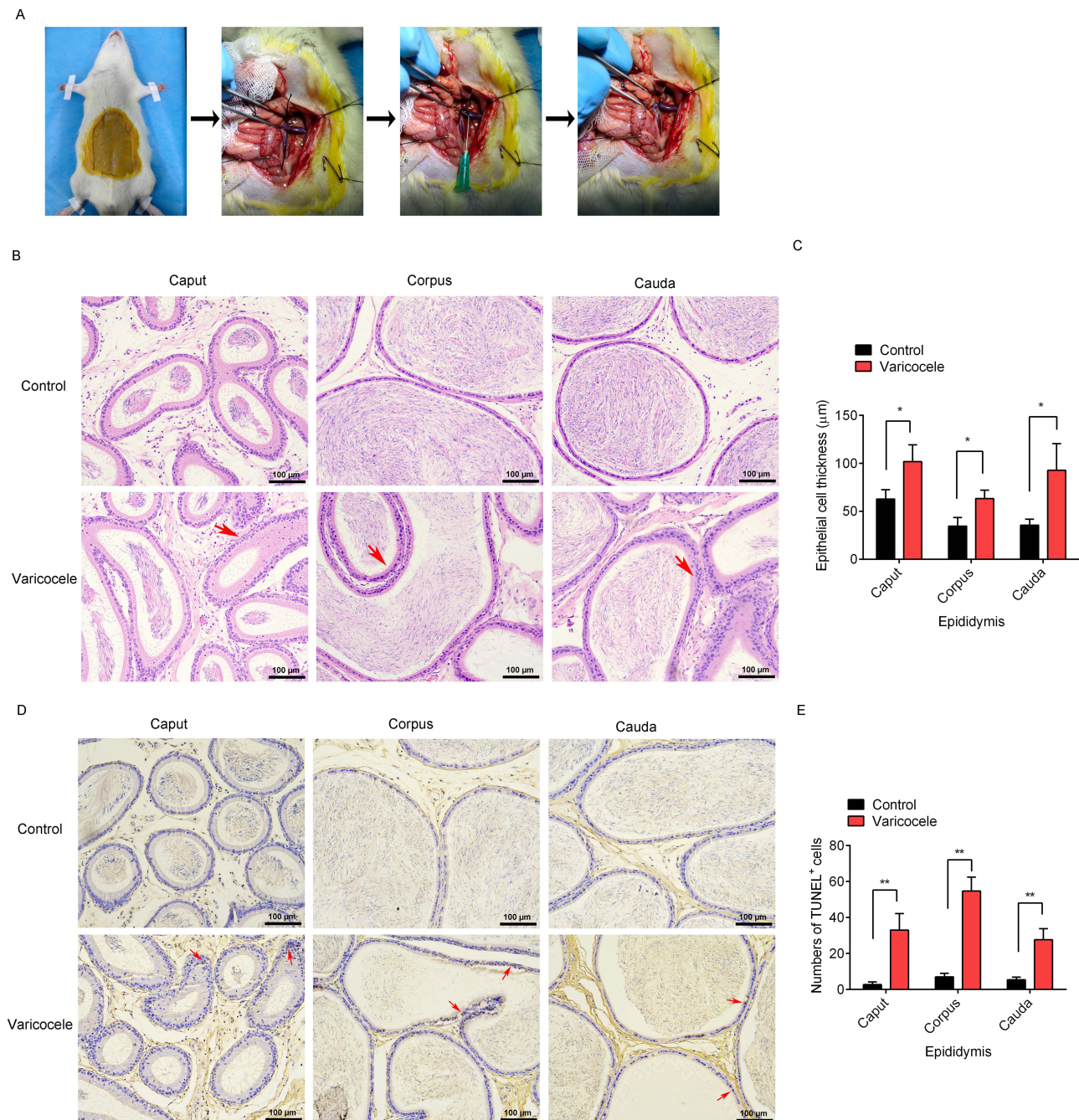
Figure 1 Effects of experimental left varicocele on the epididymal damage. (**A**) Images of the animal experiment. (**B**) H&E staining, Scale = 100 μm. (**C**) Epididymal cell thickness. (**D**) TUNEL staining, Scale = 100 μm. (**E**) Numbers of TUNEL$^+$ cells. Red arrows: hypertrophy of endothelial cells; apoptosis of endothelial cells. *$P<0.05$; **$P<0.01$.

Experimental Left Varicocele Destroyed Epididymal Function and Increased ATF-6 Expression in Epididymal Endothelial Cells

The epididymal function was assessed by measuring the NAG levels, and the expressions of NAG in the epididymal endothelial cells (black arrows) were observed by immunohistochemistry (Figure 2A). Compared with the control group, the NAG levels were significantly decreased in the caput (p=0.008), corpus (p=0.003), and cauda (p=0.004) after the experimental left varicocele (Figure 2B). The ATF-6 expressions in the epididymal endothelial cells (black arrows) were also observed by immunohistochemistry (Figure 2C). However, the ATF-6
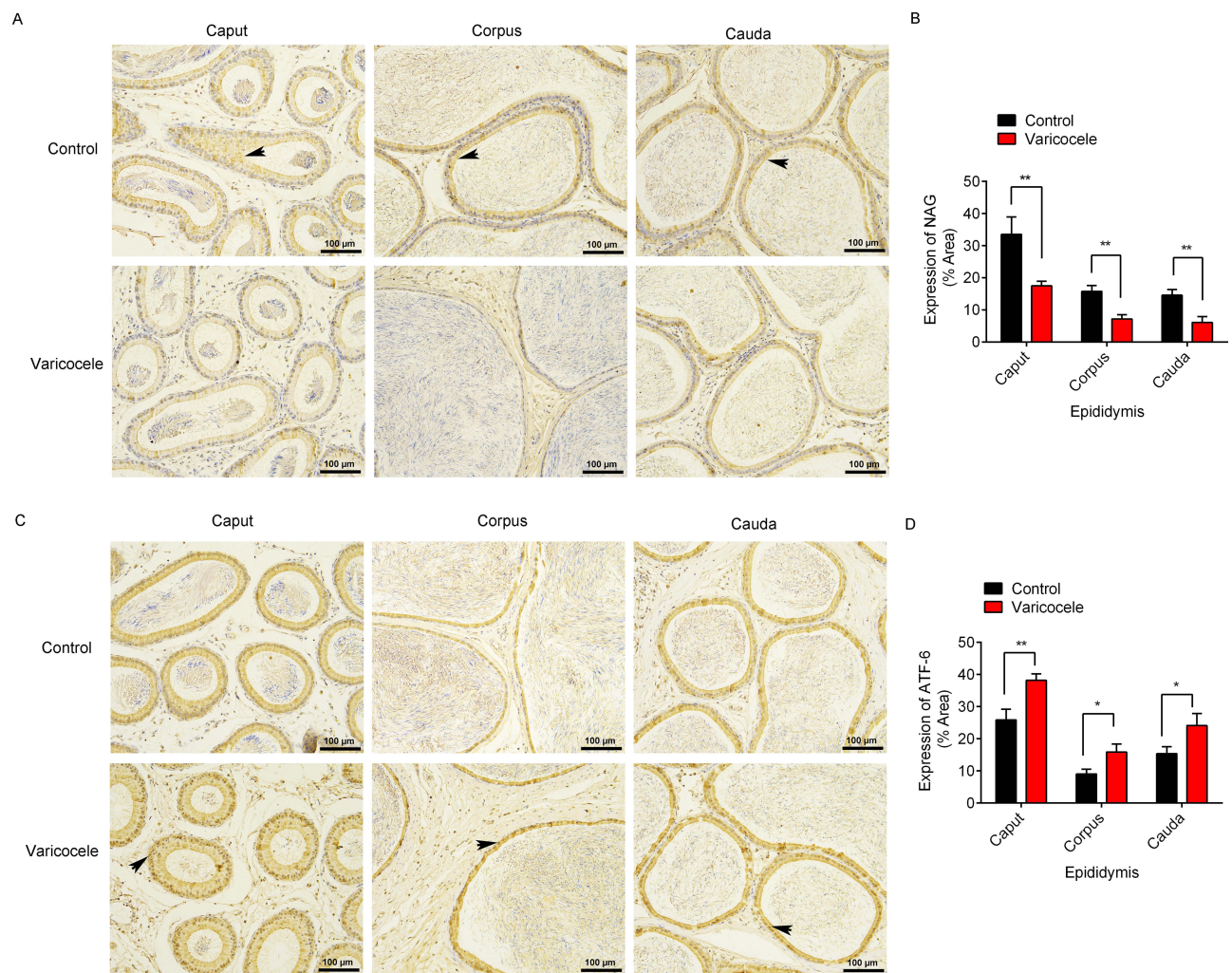
Figure 2 Effects of experimental left varicocele on the expressions of NAG and ATF-6 in the epididymis. (**A**) The expressions of NAG were observed by immunohistochemistry. Scale = 100 μm. Black arrows: positive expressions of NAG. (**B**) The area of NAG expression was analyzed using ImageJ software. (**C**) The expressions of ATF-6were observed by immunohistochemistry. Scale = 100 μm. Black arrows: positive expressions of ATF-6. (**D**) The area of ATF-6 expression was analyzed using ImageJ software. *P<0.05; **P<0.01.

expressions were significantly increased in the caput (p=0.006), corpus (p=0.015), and cauda (p=0.025) after the experimental left varicocele when compared to the control group (Figure 2D). The results showed that the experimental left varicocele destroyed the epididymal function and activated the ATF-6 pathway in the epididymal endothelial cells.

Experimental Left Varicocele Induced Inflammation in Epididymal Endothelial Cells

The inflammation in the epididymal endothelial cells was assessed by measuring the expressions of TNF-α and p-NF-κB p65 (S536), and their expressions were observed by immunohistochemistry. Compared with the control group, the TNF-α expression in the epididymal endothelial cells (Figure 3A, black arrows) was significantly increased in the caput (p=0.015), corpus (p=0.020), and cauda (p=0.013) after the experimental left varicocele (Figure 3B). The p-NF-κB p65 (S536) expression in the epididymal endothelial cells (Figure 3C, black arrows) was also significantly increased in the caput (p=0.001), corpus (p=0.001), and cauda (p=0.019) after the experimental left varicocele compared with the control group (Figure 3D). The results showed that the experimental left varicocele induced inflammation in the epididymal endothelial cells.
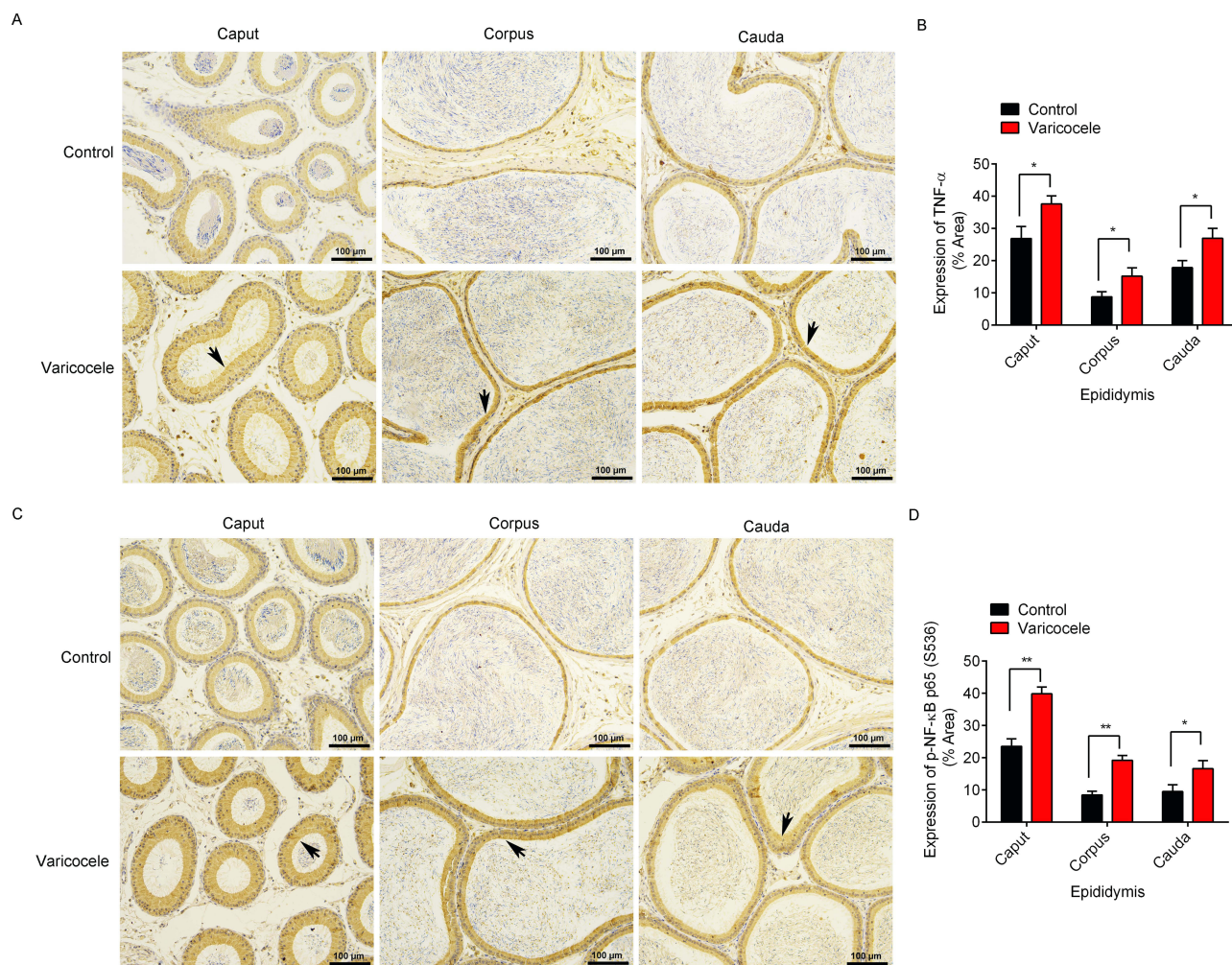
Figure 3 Effects of experimental left varicocele on the expressions of TNF-α and p-NF-κB p65 (S536) in the epididymis. The expressions of TNF-α (**A**) and p-NF-κB p65 (S536) (**C**) were observed by immunohistochemistry. Scale = 100 μm. Black arrows: positive expressions of TNF-α and p-NF-κB p65 (S536). The area of TNF-α expression (**B**) and p-NF-κB p65 (S536) expression (**D**) was analyzed using ImageJ software. *$P<0.05$; **$P<0.01$.

ATF-6 Silence Did Not Affect Epididymal Cell Function

The rat epididymal endothelial cells were identified with PCK immunofluorescence (>90%, Figure 4A). To further analyze the roles of ATF-6 in the epididymal endothelial cells, ATF-6 silence was established in the epididymal endothelial cells by ATF-6 siRNA transfection. The expressions of ATF-6 protein were observed by Western blotting (Figure 4B), and the ATF-6 siRNA transfection significantly decreased the expressions of ATF-6 protein compared with the control siRNA transfection (p=0.000). Moreover, there was no significance in the cell viability (Figure 4C, p=0.576) and NAG level (Figure 4D, p=0.909) among groups.

ATF-6 Silence Improved Hypoxia-Induced Damage in Epididymal Epithelial Cells

The control cells and ATF-6 siRNA-transfected cells were treated with hypoxia to confirm the roles of ATF-6 in the hypoxia-induced epididymal epithelial cells. Compared with the control group, the cell viability (Figure 5A, p=0.000) and NAG levels (Figure 5B, p=0.000) were significantly decreased after hypoxia treatment. Meanwhile, the cell viability (p=0.002) and NAG levels (p=0.010) in the ATF-6 siRNA group were significantly decreased after the hypoxia treatment. However, under hypoxia treatment, the ATF-6 siRNA transfection significantly increased the cell viability (p=0.000) and NAG levels (p=0.041) compared with the control cells. The levels of TNF-α (Figure 5C) and IL-8 (Figure 5D) in the cells were also measured using ELISA. Compared with the control group, the levels of TNF-α
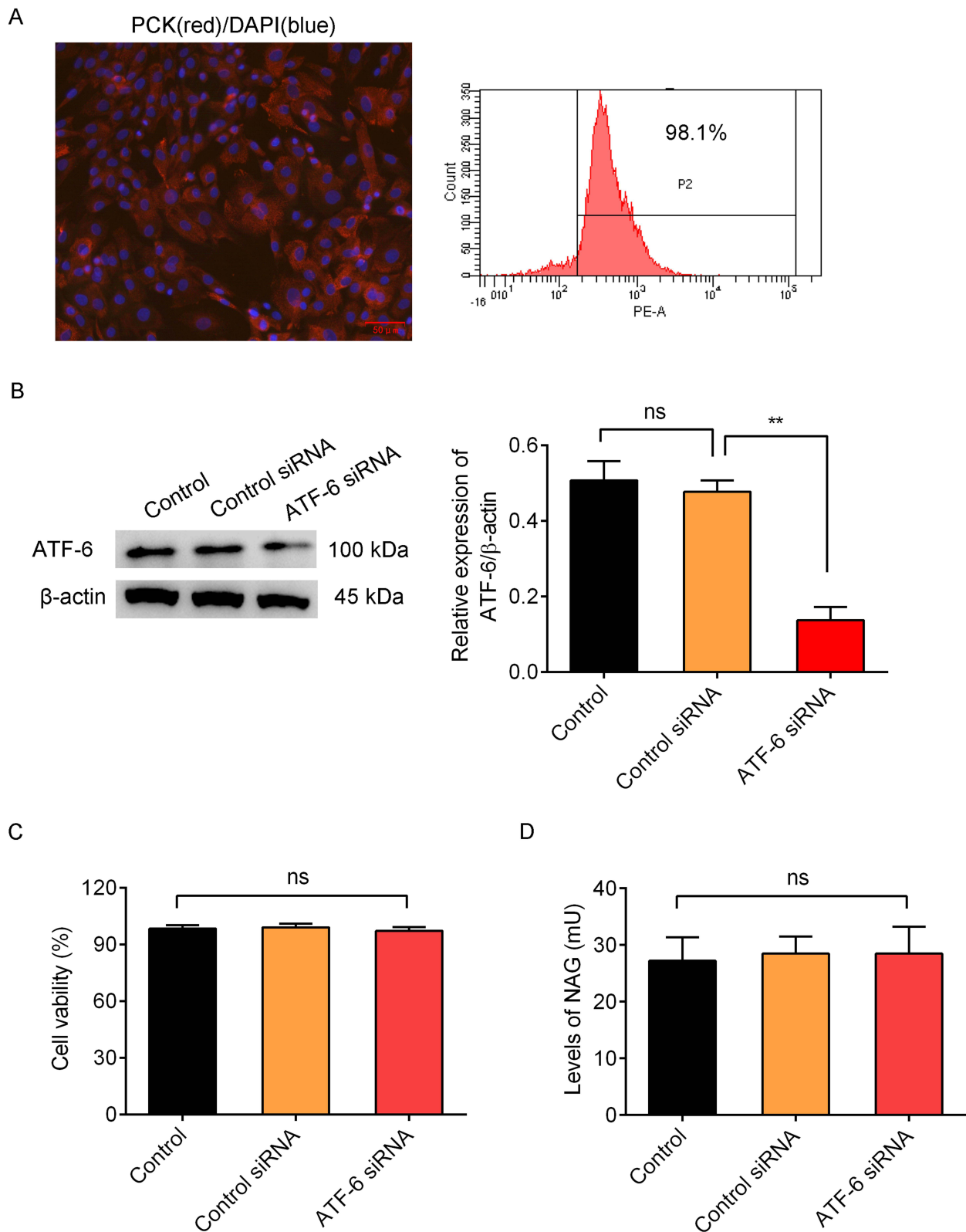
Figure 4 Effects of ATF-6 silence on cell viability and NAG level in the epididymal endothelial cells. (**A**) The cells were identified with PCK immunofluorescence (Scale = 50 μm). (**B**) The ATF-6 protein expressions were measured by Western blotting. The gray of protein was analyzed using ImageJ software and the relative expression of proteins was normalized by β-actin. (**C**) Cell viability was measured by CCK-8. (**D**) NAG levels were measured by α-glucosidase activity assay kit. ns: no significance; **$P < 0.01$.
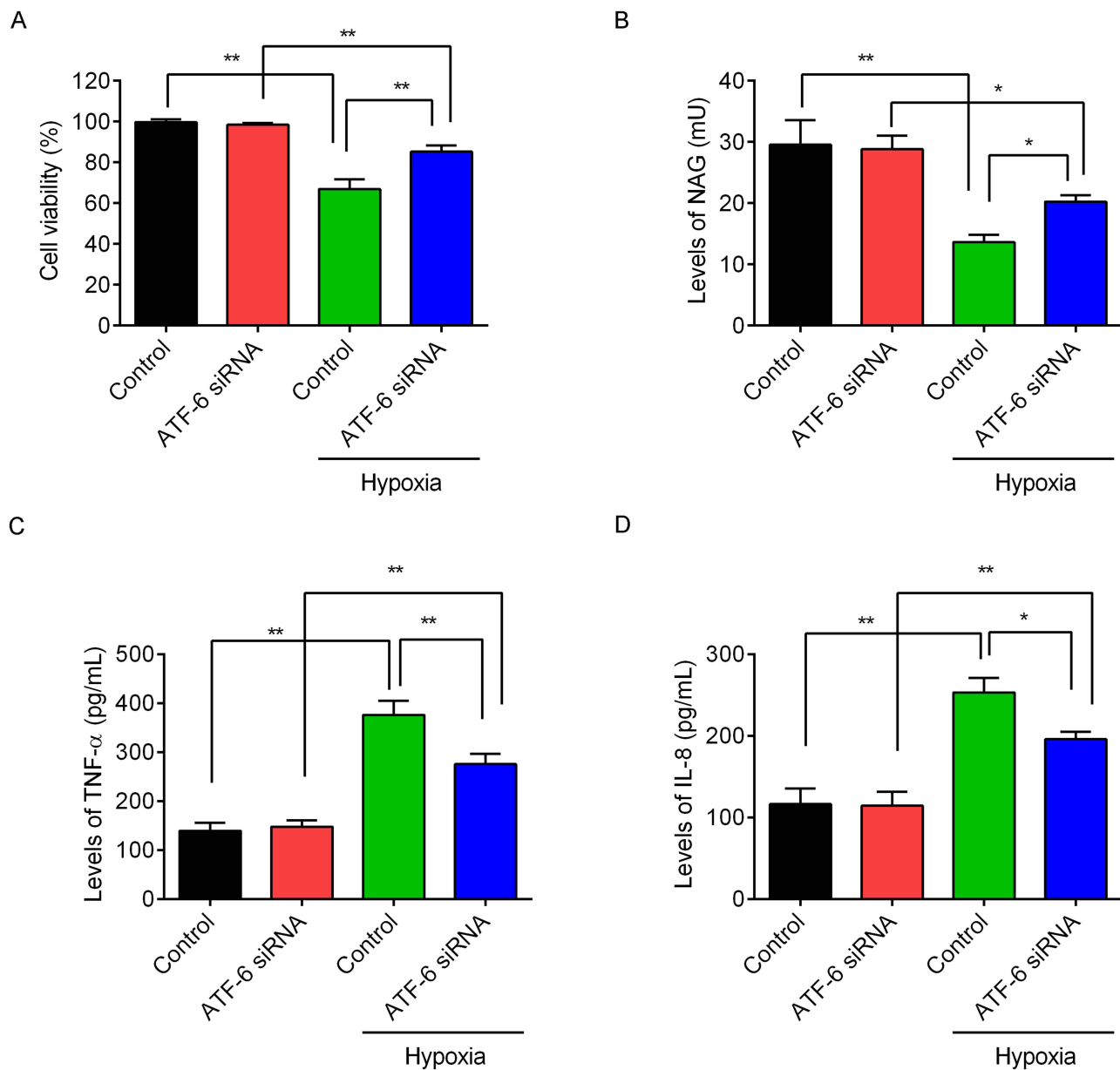
Figure 5 Effects of ATF-6 silence on the epididymal endothelial cells under hypoxia condition. The control cells and ATF-6 siRNA-transfected cells were treated with hypoxia for 24 h. (**A**) Cell viability was measured by CCK-8 kit. (**B**) Levels of NAG were measured by α-glucosidase activity assay kit. Levels of TNF-α (**C**) and IL-8 (**D**) in the supernatants were measured by ELISA kit. *$P<0.05$, **$P<0.01$.

(p=0.000) and IL-8 (p=0.000) were significantly increased after hypoxia treatment. The levels of TNF-α (p=0.000) and IL-8 (p=0.001) in the ATF-6 siRNA group were also significantly increased after hypoxia treatment. However, under hypoxia treatment, the ATF-6 siRNA transfection significantly decreased the levels of TNF-α (p=0.002) and IL-8 (p=0.011) compared with the control cells.

Moreover, the expressions of p-NF-κB p65 (S536) /NF-κB p65 protein (Figure 6A) were measured by Western blotting, and hypoxia treatment significantly increased expressions of p-NF-κB p65 (S536) /NF-κB p65 protein compared with the control group (p=0.000) or ATF-6 siRNA group (p=0.000). However, under hypoxia treatment, the ATF-6 siRNA transfection significantly decreased the expressions of p-NF-κB p65 (S536) /NF-κB p65 protein compared with the control cells (p=0.000). These results showed that ATF-6 silence improved the inflammation in the hypoxia-treated epididymal epithelial cells.
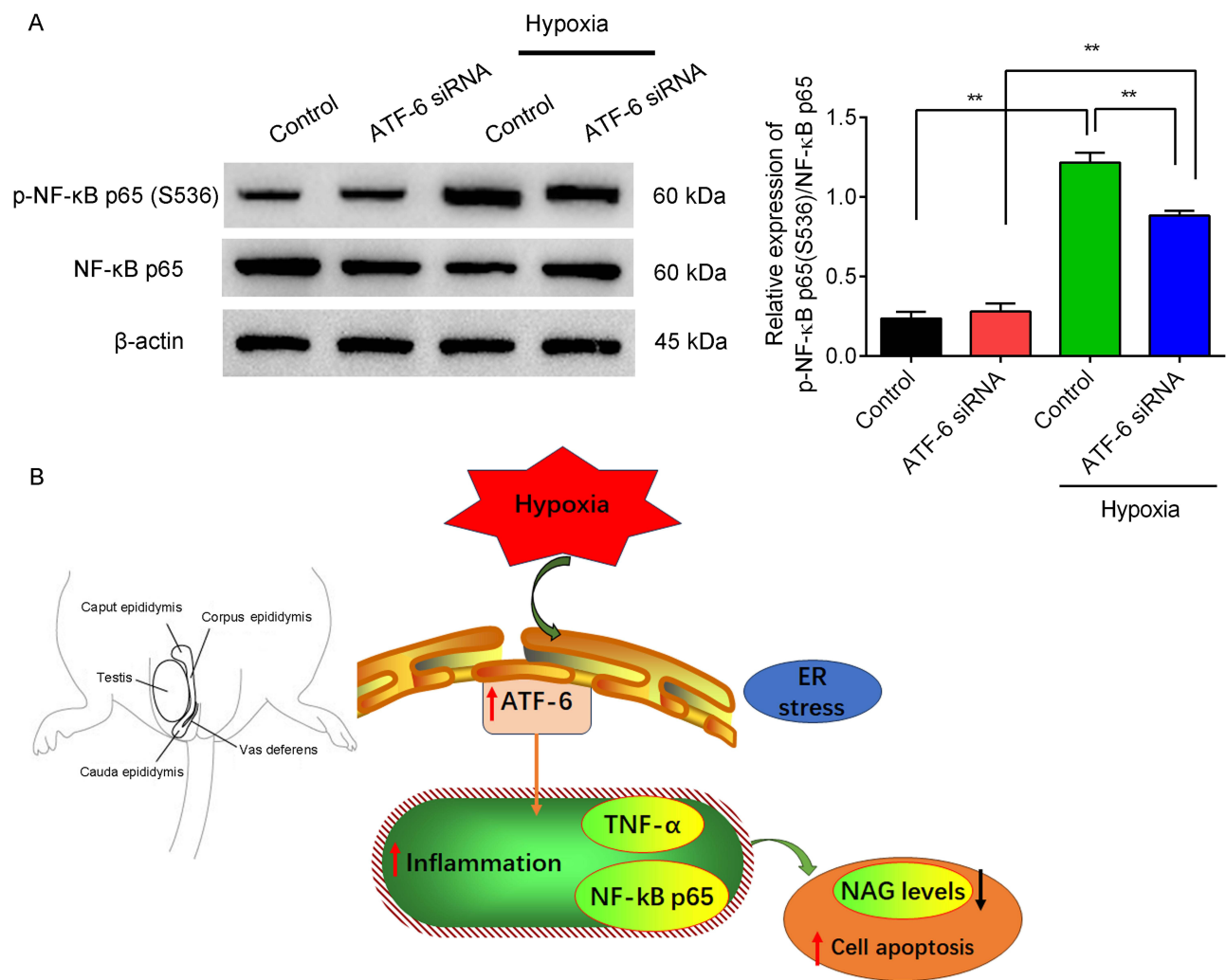
Figure 6 Effects of ATF-6 silence on the expressions of p-NF-κB p65(S536) /NF-κB p65 protein in the epididymal endothelial cells under hypoxia condition. (**A**) Expressions of p-NF-κB p65 (S536) /NF-κB p65 protein were measured by Western blotting. The gray of protein was analyzed using ImageJ software and the relative expression of proteins was normalized by β-actin. (**B**) A diagram of this study. ATF-6 mediated inflammation in experimental varicocele-induced epididymal epithelial cells. ***P<0.01.*

Discussion

The epididymis is divided into the caput, corpus, and cauda epididymis in laboratory rodents.[7,25] In this study, the experimental left varicocele induced left epididymal dysfunction by inducing cell apoptosis and inflammation and increased the ATF-6 expression in the left epididymis. Moreover, the ATF-6 mediated the hypoxia-induced inflammation in epididymal epithelial cells (Figure 6B).

The caput epididymis supports sperm maturation, and the cauda epididymis plays a role in sperm storage. The enzyme NAG is a functional epididymal marker in humans, originating almost exclusively from the epididymis.[25] Many studies have demonstrated that the epididymal structures and functions are influenced by varicocele.[9,26] The varicocele results in the decrease of sperm parameters, significant histological damage, and high levels of oxidative stress and apoptosis in the epididymis. Consistent with these findings, our study showed that the left varicocele induced epididymal damage by decreasing the NAG levels and increasing the cell apoptosis in the epididymis. Importantly, the left varicocele induced the expressions of ATF-6, TNF-α and p-NF-κB p65 (S536) increased in the epididymis, indicating that ATF-6-mediated inflammation played a vital role in the left varicocele-induced epididymal damage.

ATF-6, a transduction molecule in the downstream signal pathway of UPR, mediates ER stress. Under basal conditions, the ATF-6 pathway is inactive by binding to the ER protein chaperone BiP/GRP78. During the ER stress, increased protein load in the ER triggers the BiP/GRP78 dissociation from the UPR sensors, resulting in the ATF-6

pathway activation.[16,27] Activation of the ATF-6 pathway can increase the secretion of inflammatory cytokines in response to ER stress.[14] In a rat varicocele testis model, ER stress and unfolded protein response occurred in the testis as evidenced by the engagement of the IRE1/JNK/XBP1s pathway and caspase-3-mediated apoptosis.[11] Consistent with previous findings, this study found the ATF-6 pathway was activated in the experimental left varicocele-induced epididymis. Moreover, the inflammatory cytokines, TNF-α and p-NF-κB p65 (S536), were significantly increased in the varicocele-induced epididymis.

NF-κB transcription factors, including five members named p65 (RELA), RELB, REL, NF-κB1(p105/p50), and NF-κB2 (p/100/p52), play central roles in coordinating immune and inflammation responses.[28–30] All five members form homo- or heterodimers, among which p65/p50 is the most common one. Inflammatory cytokines can activate the NF-κB pathway, resulting in the p65/p50 complexes release and free to translocate to the nucleus.[28] As an inflammatory cytokine, TNF-α can bind to its receptor TNF-R1 to activate the NF-κB pathway.[29,30] Moreover, the ATF-6 mediates the NF-κB pathway in intestinal epithelial cells upon endoplasmic reticulum stress.[16] To confirm that ATF-6 mediates the inflammation in the left varicocele-induced epididymal damage, we established ATF-6 silence in rat epididymal endothelial cells and treated the cells with hypoxia. As known, hypoxia is one of the mechanisms of varicocele injury.[31] The results showed that the ATF-6 silence improved the hypoxia-induced inflammation by suppressing the TNF-α, IL-8, and p-NF-κB p65 (S536)/NF-κB p65 expression. These results indicated that the ATF-6-mediated inflammation participated in the varicocele-induced epididymis injury. Inhibition of the ATF-6 pathway might be a possible novel therapeutic approach for the left varicocele-induced epididymal damage.

However, many limitations of this study were not neglected. Many potential confounding factors, such as variations in rats handling or differences in individual responses to the induced varicocele, could influence the results. Besides, individual variation is one of the major difficulties of the study of venous anatomy in both humans and laboratory animals. There are currently several hypotheses related to the impairment of spermatogenesis seen in patients with varicocele, but it appears to be multifactorial with no single disturbance able to completely explain the mechanism of impairment.[32] The animal model is critical to researchers investigating the pathophysiology of varicocele. This study only explained the ATF-6 mediated inflammation in experimental varicocele-induced epididymal damage but did not explore the underlying mechanisms in detail. It is known that ATF-6 may activate other signaling pathways, such as autophagy,[33] metabolic changes,[34] and immune infiltration.[35] It is necessary to elucidate the cross-talks that occur among ATF-6-mediated pathways in the experimental left varicocele. Moreover, other potential pathways could also contribute to inflammation in varicocele-induced epididymal damage, such as oxidative damage,[36] PI3K/Akt pathway,[6] and DNA damage.[37] Other mechanisms are equally important to characterize the varicocele-induced epididymal damage.

Conclusions

This study demonstrated that the ATF-6 mediated inflammation in a rat left varicocele-induced epididymal damage, and the ATF-6 silence suppressed the hypoxia-induced inflammation in epididymal epithelial cells. Inhibition of the ATF-6 pathway might be a possible novel therapeutic approach for the left varicocele-induced epididymal damage. While the study discusses the basic science aspects, it could go further in exploring the potential clinical implications. The data of this study provide a fertile ground for future explorations.

Data Sharing Statement

The datasets generated during the current study are available from the corresponding author.

Ethical Approval

This study was approved by the Animal Care and Ethics Committee of Yantai Yuhuangding Hospital (No. 2023-417; Approval date, December 28, 2023). All experimental procedures were performed following the National Institutes of Health guide for the care and use of laboratory animals (NIH Publications No. 8023, revised 1978), and comply with the ARRIVE guidelines.

Author Contributions

All authors made a significant contribution to the work reported, whether that is in the conception, study design, execution, acquisition of data, analysis and interpretation, or in all these areas; took part in drafting, revising or critically reviewing the article; gave final approval of the version to be published; have agreed on the journal to which the article has been submitted; and agree to be accountable for all aspects of the work.

Funding

Disclosure

The authors declared no potential competing interest.

References

1. Alsaikhan B, Alrabeeah K, Delouya G, Zini A. Epidemiology of varicocele. *Asian J Androl*. 2016;18(2):179–181. doi:10.4103/1008-682x.172640
2. Jensen CFS, Østergren P, Dupree JM, Ohl DA, Sønksen J, Fode M. Varicocele and male infertility. *Nat Rev Urol*. 2017;14(9):523–533. doi:10.1038/nrurol.2017.98
3. Fang Y, Su Y, Xu J, et al. Varicocele-Mediated Male Infertility: from the Perspective of Testicular Immunity and Inflammation. *Front Immunol*. 2021;12:729539. doi:10.3389/fimmu.2021.729539
4. Pogorelić Z, Poljak K, Jukić M, Vukojević K. Ultrasonic Scalpel vs. Polymeric Clip Laparoscopic Varicocelectomy in Adolescents with Symptomatic Varicocele. *J Clin Med*. 2024;13(15):4322. doi:10.3390/jcm13154322
5. Pogorelić Z, Sopta M, Jukić M, Nevešćanin A, Jurić I, Furlan D. Laparoscopic Varicocelectomy Using Polymeric Ligating Clips and Its Effect on Semen Parameters in Pediatric Population with Symptomatic Varicocele: a 5-Year Single Surgeon Experience. *J Laparoendosc Adv Surg Tech A*. 2017;27(12):1318–1325. doi:10.1089/lap.2017.0439
6. Xia YQ, Ning JZ, Cheng F, et al. GYY4137 a H(2)S donor, attenuates ipsilateral epididymis injury in experimentally varicocele-induced rats via activation of the PI3K/Akt pathway. *Iran J Basic Med Sci*. 2019;22(7):729–735. doi:10.22038/ijbms.2019.30588.7372
7. Sullivan R, Légaré C, Lamontagne-Proulx J, Breton S, Soulet D. Revisiting structure/functions of the human epididymis. *Andrology*. 2019;7(5):748–757. doi:10.1111/andr.12633
8. Chen Q, Zhou R, Yang C, et al. Ergothioneine attenuates varicocele-induced testicular damage by upregulating HSP90AA1 in rats. *J Biochem Mol Toxicol*. 2023;37(4):e23301. doi:10.1002/jbt.23301
9. Vivas-Acevedo G, Lozano-Hernández R, Camejo MI. Varicocele decreases epididymal neutral α-glucosidase and is associated with alteration of nuclear DNA and plasma membrane in spermatozoa. *BJU Int*. 2014;113(4):642–649. doi:10.1111/bju.12523
10. Li JP, Zhang XZ, Wu JG, et al. Seminal plasma neutral alpha-glucosidase activity as an early predictor of patency and natural pregnancy after microsurgical vasoepididymostomy. *Andrologia*. 2019;51(5):e13235. doi:10.1111/and.13235
11. Hosseini M, Shaygannia E, Rahmani M, et al. Endoplasmic Reticulum Stress (ER Stress) and Unfolded Protein Response (UPR) Occur in a Rat Varicocele Testis Model. *Oxid Med Cell Longev*. 2020;2020:5909306. doi:10.1155/2020/5909306
12. Rahmani M, Tavalaee M, Rd J, Nasr-Esfahani MH. Role of Endoplasmic Reticulum Stress in The Male Reproductive System. *Cell J*. 2023;25(7):437–446. doi:10.22074/cellj.2023.1983074.1205
13. Li W, Cao T, Luo C, et al. Crosstalk between ER stress, NLRP3 inflammasome, and inflammation. *Appl Microbiol Biotechnol*. 2020;104(14):6129–6140. doi:10.1007/s00253-020-10614-y
14. Sullivan GP, O'Connor H, Henry CM, et al. TRAIL Receptors Serve as Stress-Associated Molecular Patterns to Promote ER-Stress-Induced Inflammation. *Dev Cell*. 2020;52(6):714–730.e715. doi:10.1016/j.devcel.2020.01.031
15. Dong B, Sun Y, Cheng B, Xue Y, Li W, Sun X. Activating transcription factor (ATF) 6 upregulates cystathionine β synthetase (CBS) expression and hydrogen sulfide (H(2)S) synthesis to ameliorate liver metabolic damage. *Eur J Med Res*. 2023;28(1):540. doi:10.1186/s40001-023-01520-w
16. Stengel ST, Fazio A, Lipinski S, et al. Activating Transcription Factor 6 Mediates Inflammatory Signals in Intestinal Epithelial Cells Upon Endoplasmic Reticulum Stress. *Gastroenterology*. 2020;159(4):1357–1374.e1310. doi:10.1053/j.gastro.2020.06.088
17. Lei Y, Yu H, Ding S, Liu H, Liu C, Fu R. Molecular mechanism of ATF6 in unfolded protein response and its role in disease. *Heliyon*. 2024;10(5):e25937. doi:10.1016/j.heliyon.2024.e25937
18. Yilmaz S, Gur C, Kucukler S, Akaras N, Kandemir FM. Zingerone attenuates sciatic nerve damage caused by sodium arsenite by inhibiting NF-κB, caspase-3, and ATF-6/CHOP pathways and activating the Akt2/FOXO1 pathway. *Iran J Basic Med Sci*. 2024;27(4):485–491. doi:10.22038/ijbms.2023.74088.16094
19. Turner TT, Howards SS. The venous anatomy of experimental left varicocele: comparison with naturally occurring left varicocele in the human. *Fertil Steril*. 1994;62(4):869–875. doi:10.1016/s0015-0282(16)57018-6
20. Ozturk U, Kefeli M, Asci R, Akpolat I, Buyukalpelli R, Sarikaya S. The effects of experimental left varicocele on the epididymis. *Syst Biol Reprod Med*. 2008;54(4–5):177–184. doi:10.1080/19396360802415752
21. Feldman AT, Wolfe D. Tissue processing and hematoxylin and eosin staining. *Methods Mol Biol*. 2014;1180:31–43. doi:10.1007/978-1-4939-1050-2_3
22. Hussaini HM, Seo B, Rich AM. Immunohistochemistry and Immunofluorescence. *Methods Mol Biol*. 2023;2588:439–450. doi:10.1007/978-1-0716-2780-8_26
23. Sule R, Rivera G, Gomes AV. Western blotting (immunoblotting): history, theory, uses, protocol and problems. *Biotechniques*. 2023;75(3):99–114. doi:10.2144/btn-2022-0034

24. Wang H, Zhu B, Jing T, et al. Lycopene inhibits apoptosis of mouse spermatocytes in varicocele via miR-23a/b-induced downregulation of PROK2. *Reprod Fertil Dev*. 2024;36(4). doi:10.1071/rd23136

25. James ER, Carrell DT, Aston KI, Jenkins TG, Yeste M, Salas-Huetos A. The Role of the Epididymis and the Contribution of Epididymosomes to Mammalian Reproduction. *Int J Mol Sci*. 2020;21(15):5377. doi:10.3390/ijms21155377

26. Fallah Asl H, Jalali Mashayekhi F, Zendedel A, Baazm M. The time course of nod-like receptor family pyrin domain containing 3 inflammasome complex expressions in the testis tissue of an experimental varicocele rat model: an experimental study. *Int J Reprod Biomed*. 2023;21(7):577–584. doi:10.18502/ijrm.v21i7.13895

27. Yardim A, Kandemir FM, Ozdemir S, et al. Quercetin provides protection against the peripheral nerve damage caused by vincristine in rats by suppressing caspase 3, NF-κB, ATF-6 pathways and activating Nrf2, Akt pathways. *Neurotoxicology*. 2020;81:137–146. doi:10.1016/j.neuro.2020.10.001

28. Capece D, Verzella D, Flati I, Arboretto P, Cornice J, Franzoso G. NF-κB: blending metabolism, immunity, and inflammation. *Trends Immunol*. 2022;43(9):757–775. doi:10.1016/j.it.2022.07.004

29. Bao HL, Chen CZ, Ren CZ, et al. Polydatin ameliorates hepatic ischemia-reperfusion injury by modulating macrophage polarization. *Hepatobiliary Pancreat Dis Int*. 2024;23(1):25–34. doi:10.1016/j.hbpd.2022.08.009

30. Huang Z, Mou T, Luo Y, et al. Inhibition of miR-450b-5p ameliorates hepatic ischemia/reperfusion injury via targeting CRYAB. *Cell Death Dis*. 2020;11(6):455. doi:10.1038/s41419-020-2648-0

31. Wang H, Zhu B, Yu L, et al. Lycopene Attenuates Hypoxia-Induced Testicular Injury by Inhibiting PROK2 Expression and Activating PI3K/AKT/mTOR Pathway in a Varicocele Adult Rat. *Evid Based Complement Alternat Med*. 2021;2021:3471356. doi:10.1155/2021/3471356

32. Katz MJ, Najari BB, Li PS, Goldstein M. The role of animal models in the study of varicocele. *Transl Androl Urol*. 2014;3(1):59–63. doi:10.3978/j.issn.2223-4683.2014.01.07

33. Das B, Samal S, Hamdi H, et al. Role of endoplasmic reticulum stress-related unfolded protein response and its implications in dengue virus infection for biomarker development. *Life Sci*. 2023;329:121982. doi:10.1016/j.lfs.2023.121982

34. Senkal CE, Ponnusamy S, Manevich Y, et al. Alteration of ceramide synthase 6/C16-ceramide induces activating transcription factor 6-mediated endoplasmic reticulum (ER) stress and apoptosis via perturbation of cellular Ca2+ and ER/Golgi membrane network. *J Biol Chem*. 2011;286 (49):42446–42458. doi:10.1074/jbc.M111.287383

35. Cakmak F, Kucukler S, Gur C, Comakli S, Ileriturk M, Kandemir FM. Morin provides therapeutic effect by attenuating oxidative stress, inflammation, endoplasmic reticulum stress, autophagy, apoptosis, and oxidative DNA damage in testicular toxicity caused by ifosfamide in rats. *Iran J Basic Med Sci*. 2023;26(10):1227–1236. doi:10.22038/ijbms.2023.71702.15580

36. Missassi G, Dos Santos Borges C, de Lima Rosa J, et al. Chrysin Administration Protects against Oxidative Damage in Varicocele-Induced Adult Rats. *Oxid Med Cell Longev*. 2017;2017(1):2172981. doi:10.1155/2017/2172981

37. Moshari S, Razi M, Nasr-Esfahani MH, Tavalaee M, Hajian M. Experimental Varicocele Impairs DNA Methylation and Demethylation in Germ Cells, TESE, and Epididymal Spermatozoa, Impacting Active DNA Demethylation in Zygotes. *Reprod Sci*. 2024. doi:10.1007/s43032-024-01651-3